Vibrational spectroscopy (FT-IR and FT-Raman) investigation, and hybrid computational (HF and DFT) analysis on the structure of 2,3-naphthalenediol

ARTICLE *in* SPECTROCHIMICA ACTA PART A MOLECULAR AND BIOMOLECULAR SPECTROSCOPY · SEPTEMBER 2011

Impact Factor: 2.35 · DOI: 10.1016/j.saa.2011.09.002 · Source: PubMed

4 AUTHORS, INCLUDING:

Sengeny Periandy
Independent Researcher
83 PUBLICATIONS **685** CITATIONS
SEE PROFILE

Mehmet Karabacak
Celal Bayar Üniversitesi
131 PUBLICATIONS **1,484** CITATIONS
SEE PROFILE

S. Ramalingam
A.V.C. College (Autonomous)
72 PUBLICATIONS **386** CITATIONS
SEE PROFILE

Spectrochimica Acta Part A 83 (2011) 540–552

Contents lists available at SciVerse ScienceDirect

Spectrochimica Acta Part A: Molecular and Biomolecular Spectroscopy

journal homepage: www.elsevier.com/locate/saa

Vibrational spectroscopy (FT-IR and FT-Raman) investigation, and hybrid computational (HF and DFT) analysis on the structure of 2,3-naphthalenediol

D. Shoba [a,b], S. Periandy [c], M. Karabacak [d], S. Ramalingam [e,*]

[a] Periyar Maniyammai University, Thanjavur, Tamilnadu, India
[b] Department of Physics, Alpha College of Engineering & Technology, Puducherry, India
[c] Department of Physics, Tagore Arts College, Puducherry, India
[d] Department of Physics, Afyon Kocatepe University, Afyonkarahisar, Turkey
[e] Department of Physics, A.V.C. College, Mayiladuthurai, Tamilnadu, India

ARTICLE INFO

Article history:
Received 3 August 2011
Received in revised form 19 August 2011
Accepted 1 September 2011

Keywords:
2,3-Naphthalenediol
HOMO–LUMO
Frontier molecular orbital energies
Vibrational frequencies
HF and DFT

ABSTRACT

The FT-IR and FT-Raman vibrational spectra of 2,3-naphthalenediol ($C_{10}H_8O_2$) have been recorded using Bruker IFS 66V spectrometer in the range of 4000–100 cm^{-1} in solid phase. A detailed vibrational spectral analysis has been carried out and the assignments of the observed fundamental bands have been proposed on the basis of peak positions and relative intensities. The optimized molecular geometry and vibrational frequencies in the ground state are calculated by using the ab initio Hartree–Fock (HF) and DFT (LSDA and B3LYP) methods with 6-31+G(d,p) and 6-311+G(d,p) basis sets. There are three conformers, C1, C2 and C3 for this molecule. The computational results diagnose the most stable conformer of title molecule as the C1 form. The isotropic computational analysis showed good agreement with the experimental observations. Comparison of the fundamental vibrational frequencies with calculated results by HF and DFT methods. Comparison of the simulated spectra provides important information about the capability of computational method to describe the vibrational modes. A study on the electronic properties, such as absorption wavelengths, excitation energy, dipole moment and Frontier molecular orbital energies, are performed by time dependent DFT approach. The electronic structure and the assignment of the absorption bands in the electronic spectra of steady compounds are discussed. The calculated HOMO and LUMO energies show that charge transfer occurs within the molecule. On the basis of the thermodynamic properties of the title compound at different temperatures have been calculated. The statistical thermodynamic properties (standard heat capacities, standard entropies, and standard enthalpy changes) and their correlations with temperature have been obtained from the theoretical vibrations.

1. Introduction

The naphthalene and its derivatives are the most important class of organic compounds. Because of their spectroscopic properties and chemical significance, naphthalene and its derivatives were studied extensively by spectroscopic and theoretical methods. The structure of naphthalene is benzene like, having two six membered rings fused together. They are biologically, pharmaceutically and industrially useful compounds. Vibrational spectra carry significant information about structure, potential energy surfaces and interaction with environment. Molecular vibrations have attracted much attention from both experimental and theoretical communities. Modern vibrational spectrometry has proven to be an exceptionally powerful technique for solving many chemical problems. It has been extensively employed both in the study of chemical kinetics and chemical analysis. However for a proper understanding of IR and Raman, a reliable assignment of all vibrational bands is essential. Recently computational methods based on density functional theory (DFT) become widely used. This method predicts relatively accurate molecular structure and vibrational spectra with moderate computational effort [1–5].

Dihydroxynaphthalene are compounds having two hydroxyl groups are substituted to naphthalene ring system. There are positional isomers differing by the location of the hydroxyl group. The different positions provide various chemical structures which offer important roles to each characteristic. They are used directly in making several dyes and are converted into numerous corresponding amines, esters, ethers and carboxylic derivatives as well as into numerous sulfo- and nitro-group substituted (mono-, di- and tri) compounds. They find extensive applications in making dyes, pigments, fluorescent whiteners, tanning agents, antioxidants, and antiseptics. Dihydroxynaphthalene structure is found as a fable in transition-metal catalysts particularly in the form of binaphthalenediol which is composed of two naphthalenediol rings

* Corresponding author. Tel.: +91 9003398477; fax: +91 04364 225367.
E-mail address: ramalingam.physics@gmail.com (S. Ramalingam).

1386-1425/$ – see front matter.
doi:10.1016/j.saa.2011.09.002

connected at one carbon site on each ring. 2,3-Naphthalenediol (abbreviated as 2,3-ND) is used as an intermediate for organic synthesis especially for crown ether and naphthalene sulfonic acid series used to make colorant compounds [6].

Since naphthalene and its derivatives have wide applications in the biological, pharmaceutical and industrial processes. Srivastava and Singh [7] investigated naphthalene and its cation are infrared and Raman spectrum of the condensed and liquid phase. Methoxynaphthalene was investigated the MNAP by using Wilson's F–G matrix method by Xavier et al. [8]. Nagabalasubramanian and Periandy [9] studied the FT-IR and FT-Raman vibrational spectra of 1,5-methylnaphthalene molecule. FT-IR and FT-Raman spectra of 1-methoxynapthalene were reported by Govindarajan et al. [10]. Because of less number of works in the 2,3-ND molecules, has been taken for the present study. The complete vibrational analysis of 2,3-ND was performed by combining the experimental and theoretical information using Pulay's DFT based on scaled quantum chemical approach [11] and ab initio HF. It is expected that both ab initio HF and DFT level of theories are reliable for predicting the vibrational spectra of the title compound.

In this study, molecular geometry, optimized parameters, vibrational frequencies, HOMO (highest occupied molecular orbital) and LUMO (lowest unoccupied molecular orbital) energies, Frontier orbital energy gap, dipole moment and thermodynamic properties at various temperatures are computed and the performance of the computational methods for ab initio HF and DFT (LSDA and B3LYP) methods at 6-31+G(d,p) and 6-311+G(d,p) basis sets are compared. These methods expected relatively accurate molecular structure and vibrational spectra with moderate computational effort. In particular, for polyatomic molecules the DFT methods lead to the conventional ab initio HF calculations. In DFT methods, Becke's three parameter exact exchange-functional (B3) [12] combined with gradient-corrected correlational functional of Lee, Yang and Parr (LYP) [13,14] are the best predicting results for molecular geometry and vibrational wave numbers for moderately larger molecule [15–17]. Present vibrational and electronic studies, not only helps for the proper assignments of the observed and computed frequencies but also offers a comprehensive picture about the molecular dynamics and electronic properties of 2,3-ND molecule.

2. Experimental details

The compound under investigation namely 2,3-ND is purchased from Sigma–Aldrich chemicals, USA, which is of spectroscopic grade and hence used for recording the spectra as such without any further purification. The FT-IR spectrum of the compound is recorded in Bruker IFS 66V spectrometer in the range of 4000–100 cm^{-1}. The spectral resolution is $\pm 2\ cm^{-1}$. The FT-Raman spectrum of same compound is also recorded in the same instrument with FRA 106 Raman module equipped with Nd:YAG laser source operating at 1.064 μm line widths with 200 mW power. The spectra are recorded in the range of 4000–100 cm^{-1} min^{-1} of spectral width 2 cm^{-1}. The frequencies of all sharp bands are accurate to $\pm 1\ cm^{-1}$.

3. Computational methods

The first task for the computational work was to determine the optimized geometry of 2,3-ND molecule. The molecular structure of the title compound in the ground state is computed by performing both ab initio HF and DFT with 6-31+G(d,p) and 6-311+G(d,p) basis sets. The optimized structural parameters are used in the vibrational frequency calculations at HF and DFT levels. The minimum energy of geometrical structure is obtained by using level 6-31+G(d,p) and 6-311+G(d,p) basis sets. At the optimized geometry for the title molecule no imaginary frequency modes were obtained, so there is a true minimum on the potential energy surface was found. All the computations have been done by adding polarization function d and diffuse function on heavy atoms [18] and polarization function p and diffuse function on hydrogen atoms [19], in addition to triple split valence basis set 6-311+G(d,p) for better treatment of hydroxyl group. Therefore, we had a discussion on calculated values using these sets. The calculated frequencies are scaled by 0.886, 0.897 and 0.905 for HF/6-31+G(d,p). For LSDA/6-31+G(d,p) set is scaled with 0.887, 0.910, 0.974, 0.960, 0.940, 1.05 and 1.130. And for LSDA/6-311+G(d,p) basis set is scaled with 0.896, 0.918, 1.08, 1.03 and 1.12. For B3LYP/6-31+G(d,p) basis set is 0.895, 0.913, 0.947, 1.001, 1.02, 1.25 and 3.04. For B3LYP/6-311+G(d,p) basis set is scaled with 0.904, 0.925, 0.992, 0.975, 1.035 and 1.15. The theoretical results have enabled us to make the detailed assignments of the experimental IR and Raman spectra of the title molecule [20]. HF and DFT calculations for 2,3-ND are performed using GAUSSIAN 09 W program package on Pentium IV processor personal computer without any constraint on the geometry [21,22]. The electronic properties, such as HOMO–LUMO energies, absorption wavelengths and oscillator strengths were calculated using B3LYP method of the time-dependent TD-DFT, basing on the optimized structure in solvent (DMSO and chloroform) and gas phase. The changes in the thermodynamic functions the heat capacity, entropy, and enthalpy were investigated for the different temperatures from the vibrational frequencies calculations of title molecule.

Table 1
Calculated energies and energy difference for three conformers of 2,3-ND by DFT.

Conformers	B3LYP6-311G(d,p)		
	Energy (hartree)	Energy (kcal/mol)	Energy differences[a] (kcal/mol)
C1	−536.47337217	−336642.13753	0.00000
C2	−536.46703799	−336638.16278	3.97476
C3	−536.46042192	−336634.01113	8.12640

[a] Energies of the other three conformers relative to the most stable C1 conformer.

4. Results and discussion

4.1. Molecular geometry

The molecular structure of the 2,3-ND belongs to Cs point group symmetry. The dihedral angle between the aromatic ring and OH group for 2,3-ND is computed ca. 0° (or ca. 180°). 2,3-ND may have three possible structures in connection with the hydrogen atom orientations of the oxygen atom of naphthalene molecule. Calculated energies and energy difference [the relative energy of the other conformers was as: $\Delta E = E(\mathrm{Cn}) - E(\mathrm{C1})$, the conformer C1 is the lowest energy as reference point] for all conformers of 2,3-ND are presented in Table 1. The conformer C1 is predicted to be from 3.97476 to 8.12640 kcal/mol more stable than the other conformers. Additionally, because of the imaginary frequency, the calculations showed the conformer C3 to be unstable conformer. Therefore, in this section, we tabulated only C1 conformer calculations data. Fig. 1 shows the optimized structure and demonstration of three possible conformations of compound along with numbering of the atoms. The optimized most stable molecular structure of title molecule is obtained from GAUSSIAN 09 W and GAUSSVIEW05 programs are shown in Fig. 2. The title molecule contains two hydroxylic group connected with naphthalene ring at 2nd and 3rd position. The structure optimization zero point vibrational energy of the title compound in HF/6-31+G(d,p), HF/6-311+G(d,p), LSDA/6-31+G(d,p), LSDA/6-311+G(d,p), B3LYP/6-31+G(d,p) and B3LYP/6-311+G(d,p)

Table 2
Optimized geometrical parameters for 2,3-naphthalenediol computed at HF, DFT (LSDA and B3LYP) methods using 6-31+G(d,p) and 6-311+G(d,p) basis sets.

Geometrical parameters[a]	Methods			Experimental value[b]
	HF/6-31G+/6-311G+ (d,p)	LSDA/6-31G+/6-311G (d,p)	B3LYP/6-31G+/6-311G+ (d,p)	
Bond length (Å)				
C1–C2	1.3547/1.3525	1.3715/1.3666	1.3746/1.3710	
C1–C6	1.4225/1.4212	1.4113/1.4079	1.4218/1.4189	
C2–C3	1.4242/1.4237	1.4185/1.4151	1.4258/1.4235	
C3–C4	1.3539/1.3517	1.3690/1.3640	1.3732/1.3696	
C4–C5	1.4234/1.4221	1.4130/1.4091	1.4233/1.4205	
C5–C6	1.4082/1.4057	1.4301/1.4259	1.4344/1.4312	1.421
C5–C10	1.4187/1.4174	1.4096/1.4058	1.4205/1.4179	
C6–C9	1.4195/1.4183	1.4111/1.4073	1.4216/1.4191	1.422
C9–C13	1.3620/1.3599	1.3763/1.3711	1.3794/1.3754	1.377
C10–C12	1.3621/1.3600	1.3766/1.3714	1.3797/1.3757	
C12–C13	1.4150/1.4140	1.4071/1.4027	1.4166/1.4136	1.41
C1–H8	1.0749/1.0748	1.0958/1.0939	1.0856/1.0839	
C4–H11	1.0775/1.0773	1.0987/1.0967	1.0883/1.0865	
C10–H14	1.0765/1.0763	1.0973/1.0952	1.0873/1.0854	
C12–H15	1.0755/1.0753	1.0954/1.0933	1.0861/1.0841	1.098
C13–H16	1.0755/1.0753	1.0955/1.0934	1.0861/1.0842	
H7–C9	1.0761/1.0759	1.0970/1.0949	1.0870/1.0850	1.095
C2–O17	1.3472/1.3457	1.3465/1.3428	1.3646/1.3623	1.369
C3–O19	1.3582/1.3569	1.3615/1.3586	1.3779/1.3760	1.369
O17–H18	0.9451/0.9427	0.9831/0.9804	0.9691/0.9660	
O19–H20	0.9431/0.9408	0.9753/0.9723	0.9656/0.9624	
Bond angle (°)				
C2–C1–C6	120.8/120.8	120.5/120.5	120.8/120.8	121.8
C1–C2–C3	119.7/119.7	119.7/119.6	119.7/119.7	119.2
C2–C3–C4	120.8/120.8	121.2/121.2	120.9/120.9	
C3–C4–C5	120.4/120.4	120.0/120.1	120.4/120.4	
C4–C5–C6	118.8/118.8	118.9/118.8	118.7/118.7	
C4–C5–C10	121.9/121.9	122.0/122.0	122.2/122.2	
C6–C5–C10	119.1/119.1	119.0/119.0	119.0/119.0	
C1–C6–C5	119.2/119.2	119.5/119.4	119.2/119.2	
C1–C6–C9	121.8/121.8	121.8/121.9	122.0/122.0	
C5–C6–-C9	118.8/118.8	118.6/118.5	118.6/118.6	
C6–C9–C13	120.8/120.8	121.0/121.0	120.9/120.9	
C5–C10–C12	120.7/120.7	120.9/120.9	120.8/120.8	
C10–C12–C13	120.1/120.1	120.1/120.1	120.1/120.1	
C9–C13–C12	120.2/120.2	120.2/120.2	120.2/120.2	
C2–C1–H8	118.9/118.9	119.1/119.1	118.9/118.8	
C6–C1–H8	120.2/120.2	120.3/120.2	120.2/120.2	
C3–C4–H11	120.1/120.0	120.5/120.5	120.1/120.1	
C5–C4–H11	119.3/119.4	119.3/119.3	119.3/119.3	
C6–C9–H7	118.8/118.8	118.4/118.4	118.7/118.7	
C5–C10–H14	119.0/119.0	118.5/118.6	118.8/118.8	
C12–C10–H14	120.2/120.2	120.4/120.4	120.2/120.2	
C10–C12–H15	120.1/120.1	120.0/120.0	120.0/120.0	
C13–C12–H15	119.6/119.6	119.8/119.8	119.7/119.7	
C9–C13–H16	120.1/120.1	119.9/119.9	120.0/120.0	
C12–C13–H16	119.6/119.6	119.8/119.7	119.7/119.6	
H7–C9–C13	120.3/120.3	120.5/120.5	120.3/120.3	
C1–C2–O17	120.7/120.7	121.9/122.1	120.5/120.6	
C3–C2–O17	119.5/119.5	118.3/118.2	119.6/119.6	
C2–C3–O19	114.3/114.3	112.9/112.9	114.1/114.1	116.6
C4–C3–O19	124.8/124.8	125.8/125.8	124.9/124.9	123.7
C2–O17–H18	110.4/110.1	107.3/106.9	108.7/108.5	
C3–O19–H20	111.9/111.7	110.9/110.9	110.7/110.6	
Dihedral angle (°)				
C6–C1–C2–C3	0.003/−0.000	−0.010/0.000	0.002/0.000	
C2–C1–C6–C5	−0.004/−0.001	−0.001/−0.000	0.000/−0.004	
C2–C1–C6–C9	−180.0/−180.0	180.0/−180.0	−180.0/179.9	
C1–C2–C3–C4	0.006/0.003	0.015/0.000	−0.000/0.006	
C2–C3–C4–C5	−0.014/−0.005	−0.008/−0.002	−0.005/−0.009	
C3–C4–C5–C6	0.013/0.003	−0.002/0.002	0.0083/0.005	
C3–C4–C5–C10	−179.9/−179.9	179.9/180.0	−179.9/−179.9	
C4–C5–C6–C1	−0.003/0.000	0.007/−0.001	−0.005/0.001	
C4–C5–C6–C9	−180.0/180.0	180.0/180.0	179.9/180.0	
C10–C5–C6–C1	180.0/179.9	−179.9/180.0	179.9/180.0	
C10–C5–C6–C9	0.003/−0.001	0.004/0.002	0.000/0.007	
C4–C5–C10–C12	180.0/−180.0	−180.0/180.0	−179.9/−179.9	
C6–C5–C10–C12	−0.003/0.001	−0.003/−0.001	0.000/−0.003	
C1–C6–C9–C13	−180.0−180.0	179.9/−180.0	−180.0/−180.0	
C5–C6–C9–C13	−0.001/0.000	−0.001/−0.002	−0.003/−0.006	
C6–C9–C13–C12	0.000/0.000	−0.001/0.000	0.003/0.001	
C5–C10–C12–C13	0.002/0.000	0.000/−0.000	−0.002/−0.002	

Table 2 (*Continued*)

Geometrical parameters[a]	Methods			Experimental value[b]
	HF/6-31G+/6-311G+ (d,p)	LSDA/6-31G+/6-311G (d,p)	B3LYP/6-31G+/6-311G+ (d,p)	
C10–C12–C13–C9	−0.000/−0.001	0.002/0.001	−0.000/0.003	
C4–C5–C10–H14	0.005/0.001	−0.005/0.000	0.004/−0.001	
C6–C5–C10–H14	−180.0/−179.9	179.9/−180.0	−179.9/−180.0	
C1–C6–C9–H7	0.003/0.001	−0.003/−0.000	0.0027/−0.003	
C5–C6–C9–H7	−179.9/−179.9	180.0/179.9	−180.0/−180.0	
C6–C9–C13–H16	180.0/−179.9	180.0/179.9	180.0/179.9	
C10–C12–C13–H16	179.99/179.9	−179.9/180.0	180.0/180.0	
C2–C3–C4–H11	179.9/179.9	179.9/179.9	179.9/179.9	
C5–C10–C12–H15	−179.9/−179.9	180.0/−180.0	−180.0/−180.0	
C1–C2–O17–H18	179.9/179.9	−179.9/180.0	179.9/180.0	
C3–C2–O17–H18	0.012/−0.008	0.0285/0.000	0.002/0.173	
C2–C3–O19–H20	179.9/179.9	180.0/179.9	179.9/179.9	
C4–C3–O19–H20	−0.051/−0.034	0.019/0.000	−0.054/−0.028	
H8–C1–C2–C3	179.9/−180.0	179.9/180.0	−180.0/−180.0	
H8–C1–C2–O17	0.005/0.003	−0.010/−0.003	0.008/0.007	
H8–C1–C6–C9	0.007/0.002	0.012/−0.004	0.001/−0.001	
H8–C1–C6–C5	−179.9/−179.9	−179.9/−180.0	180.0/−180.0	
H11–C4–C5–C6	−179.9/−179.9	−180.0/−179.9	−179.9/−180.0	
H11–C4–C5–C10	0.006/0.008	−0.006/0.000	0.001/−0.006	
H7–C9–C13–C12	179.9/−180.0	179.9/−179.9	−180.0/−180.0	
H7–C9–C13–H16	−0.002/−0.001	−0.002/−0.001	−0.000/−0.002	
H14–C10–C12–C13	179.9/−180.0	−179.9/179.9	179.9/180.0	
H14–C10–C12–H15	−0.002/−0.000	0.002/−0.001	−0.000/−0.001	
H15–C12–C13–C9	180.0/179.9	−179.9/−179.9	179.9/180.0	
H15–C12–C13–H16	−0.001/−0.001	0.000/0.003	0.000/0.007	
C6–C1–C2–O17	180.0/180.0	−180.0/179.9	180.0/−179.9	
C1–C2–C3–O19	179.9/179.9	180.0/180.0	180.0/180.0	
O17–C2–C3–C4	−180.0/−180.0	−180.0/−179.9	−180.0/179.9	
O17–C2–C3–O19	−0.020/−0.011	−0.002/0.008	−0.008/−0.009	
O19–C3–C4–C5	−180.0/180.0	−179.9/−180.0	−180.0/−180.0	
O19–C3–C4–H11	0.001/−0.001	0.004/−0.005	−0.003/0.002	

[a] For numbering of atoms refer Fig. 2.
[b] Experimental value taken from Refs. [23,24].

are 439,376.4, 397,864.9, 408,207.6, 432,141.2, 391,540.4 and 401,847.4 J/mol and 105.01347, 95.09199, 97.56397, 103.28423, 93.58039 and 96.04383 kcal/mol, respectively. Table 2 compares the calculated bond lengths, bond angles and dihedral angles with those of experimentally available from X-ray data for 2,3-ND [23,24]. As there are two hydroxyl group attached at C2 and C3 atoms the molecule can exist in variety of conformations. From the theoretical values we can find that most of the optimized bond lengths are slightly larger, as well as smaller than the experimental values due to that the theoretical calculations belongs to isolated molecules in gaseous phase and experimental results belongs to molecules in solid state. Comparing bond angles and length of B3LYP and LSDA with those of HF, some of values of B3LYP larger than the HF values the HF calculated values correlates well compared with the experimental results. In spite of the difference calculated geometric parameters represent a good approximation and they are the bases for calculating other parameter like vibrational frequency. Many authors explained the changes in the frequency or bond length of C–H bond on substitution due to change in charge distribution on the carbon atom of the benzene ring [25,26]. The comparative IR and Raman spectra of experimental and calculated HF and DFT (LSDA and B3LYP) are given in the Fig. 3(a) and (b).

The naphthalene ring appears to be little distorted with C1–C2 and C3–C4 bond lengths exactly at the substitution place ca. 1.37 Å lesser than the remaining bonds C1–C6, C5–C6, C4–C5, C2–C3, (ca. 1.42 Å). The decrease of C–C bond exactly at the substitution place C1–C2 and C3–C4 is accompanied by slightly irregular

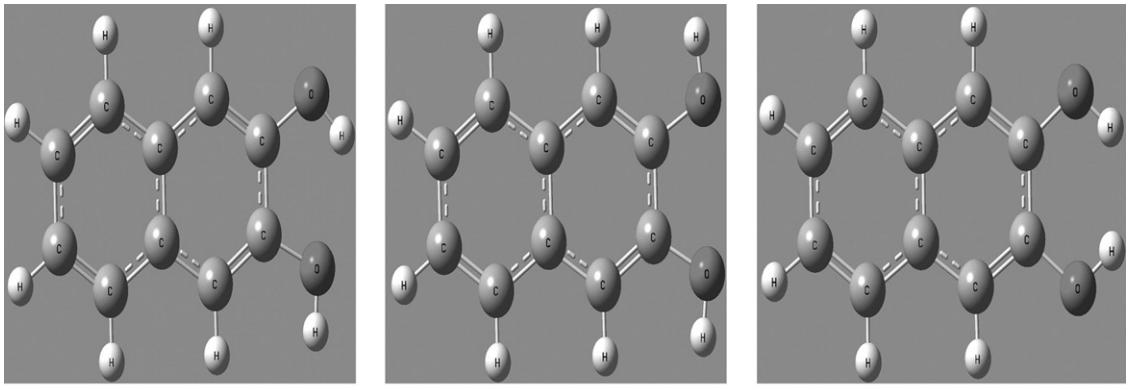

Fig. 1. The theoretical geometric structures and of 2,3-naphthalenediol (all conformers).

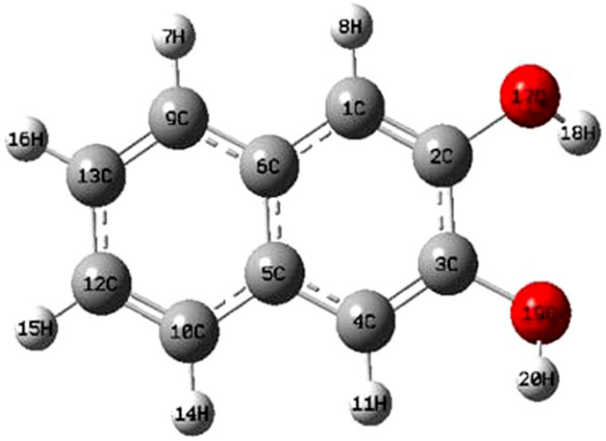

Fig. 2. Molecular structure of 2,3-naphthalenediol.

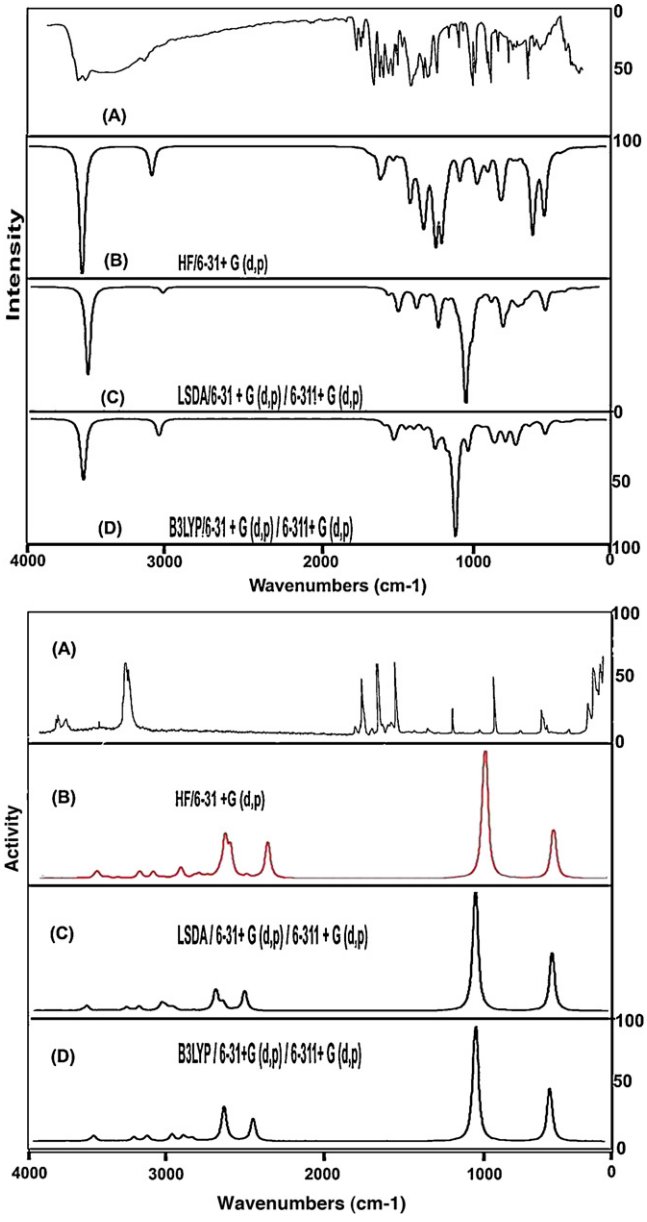

Fig. 3. (a) Experimental (A), calculated (B), (C and D) FT-IR spectra of 2,3-naphthalenediol. (b) Experimental (A), calculated (B), (C and D) FT Raman spectra of 2,3-naphthalenediol.

hexagonal structure of the angles C4–C3–O19, C2–C3–O19 and C3–C2–O17 is 124°, 114° and 119°, respectively at HF and DFT (B3LYP/6-31+G(d,p)/6-311+G(d,p) slightly differ with the experimental values. The density functional calculation gives shortening of the angle C2–C3–O19 by 6° and increasing of angle by ca. 5° from 120° at C3 position and this asymmetry of these two angles reveals the attraction between OH groups. In this present work we observed the bond angle of C4–C3–O19 is 124.8°, 125.8° and 124.9° and the bond angle of C2–C3–O19 is 114.3°, 112.9° and 114.1° for HF, LSDA and B3LYP, respectively. On comparing these two angles the former one is elongated. The bond angle of C2–C3–O19 is compressed due to elongation of C4–C3–O19 at C3 position. So that structure of naphthalene is slightly distorted.

The comparative graphs of bond lengths, bond angles and dihedral angles of title molecule for 6 sets are presented in Figs. 6–8, respectively. The optimized structure yield fairly accurate bond length pairs of C1–C10 and C6–C9, C9–C13 and C10–C12, C12–H13 and C12–H15, O17–H18 and O19–H20. At all six levels of calculation according to the experimental [23,24] the bond lengths C2–O17 and C3–O19 (1.369 Å) where as in case of DFT calculation the value of bond length C3–O19 is 0.013 Å at B3LYP 6-31+G(d,p) level, 0.015 Å at B3LYP/6-311+G(d,p) level, 0.011 Å at HF 6-31+G(d,p) level 0.015 Å at LSDA 6-31+G(d,p) level greater than C2–O17. On comparing the experimentally available bond length and bond angle with computational value, it is clear that DFT (B3LYP) estimation is better then HF which under estimate the bond length and bond angle.

4.2. Vibrational assignments

The title molecule consists of 20 atoms, which undergoes 54 normal modes of vibrations. Of the 54 normal modes of vibrations, 33 modes of vibrations are in plane and remaining 21 are out of plane. The bands that are in the plane of the molecule is represented as A′ and out-of-plane as A″. Thus the 54 normal modes of vibrations title molecule are distributed as $\Gamma_{Vib} = 33A' + 21A''$. In agreement with Cs symmetry all the 54 fundamental vibrations are active in both Raman scattering and IR absorption. The harmonic–vibrational frequencies calculated for 2,3-ND at HF and DFT (LSDA and B3LYP) levels using the triple split valence basis set along with the diffuse and polarization functions, 6-31+G(d,p) and 6-311+G(d,p) observed FT-IR and FT-Raman frequencies for various modes of vibrations have been presented in Table 3.

Comparison of frequencies calculated at HF, DFT (LSDA and B3LYP) with the experimental values reveals the over estimation of the calculated vibrational modes due to the neglect of anharmonicity in real system. Inclusion of electron correlation in the DFT to certain extends makes the frequency values bigger in the comparison with the HF frequency data. Reduction in the computed harmonic vibrations, although basis set sensitive are only marginal as observed in the DFT (B3LYP) values using 6-31+G(d,p) any way notwithstanding the level of calculations, it is customary to scale down the calculated harmonic frequencies in order to develop the agreement with the experiment. The scaled calculated frequencies minimize the root-mean square difference between calculated and experimental frequencies for bands with definite identifications. The descriptions concerning the assignment have also been indicated in Table 3.

4.3. Computed IR intensity and Raman activity analysis

Computed vibrational spectral IR intensities and Raman activities of the 2,3-ND molecule for corresponding wave numbers by HF and DFT (LSDA and B3LYP) methods at 6-31+G(d,p) and 6-311+G(d,p) basis set have been presented in Table 4. The title molecule belongs to Cs point group. Comparison of IR intensities

Table 3
Observed and HF and DFT (LSDA and B3LYP) methods calculated vibrational frequencies of 2,3-naphthalenediol.

S. no.	Symmetry species Cs	Observed frequency		Calculated frequency (cm^{-1}) with HF/6-31+G(d,p)		Calculated frequency (cm^{-1}) with LSDA/6-31G+(d,p)/6-311G+(d,p)		Calculated frequency (cm^{-1}) with B3LYP/6-31G+G(d,p)/6-311G+(d,p)		Vibrational assignments
		FT-IR	FT Raman	Unscaled value	Scaled value	Unscaled value	Scaled value	Unscaled value	Scaled value	
1	A′	3510vs	3510m	3960	3508	3955/3911	3504/3504	3921/3879	3509/3507	(O–H) υ
2	A′	3500vs	3500m	3959	3507	3953/3904	3502/3498	3919/3868	3508/3497	(O–H) υ
3	A′	3080w	–	3425	3072	3376/3341	3072/3067	3356/3321	3064/3072	(C–H) υ
4	A′	–	3070vs	3419	3067	3373/3338	3069/3064	3351/3317	3059/3068	(C–H) υ
5	A′	3060w	3060vs	3414	3062	3368/3333	3065/3060	3347/3312	3056/3064	(C–H) υ
6	A′	3050w	–	3407	3056	3361/3328	3059/3055	3339/3307	3049/3059	(C–H) υ
7	A′	3040w	3040vs	3402	3051	3358/3326	3056/3053	3335/3304	3045/3056	(C–H) υ
8	A′	–	3030vs	3393	3043	3352/3319	3050/3047	3328/3296	3038/3049	(C–H) υ
9	A′	1680vw	–	1872	1679	1720/1612	1675/1659	1754/1653	1660/1640	(C=C) υ
10	A′	1630s	1630w	1816	1629	1693/1610	1625/1610	1720/1643	1629/1630	(C=C) υ
11	A′	1610s	1610w	1812	1625	1690/1538	1622/1584	1716/1580	1625/1567	(C=C) υ
12	A′	1530vs	–	1717	1540	1575/1519	1534/1519	1607/1560	1522/1548	(C=C) υ
13	A′	1460vs	1460w	1631	1463	1562/1449	1468/1449	1559/1486	1476/1474	(C–C) υ
14	A′	1450vs	–	1623	1456	1515/1396	1454/1466	1528/1441	1447/1429	(C–C) υ
15	A′	1390vs	–	1556	1396	1490/1383	1430/1383	1502/1425	1371/1414	(C–C) υ + (O–H)δ
16	A′	1365vs	1365vs	1519	1362	1441/1337	1355/1377	1496/1354	1366/1343	(C–C) υ
17	A′	1330m	–	1486	1333	1352/1317	1316/1317	1401/1317	1327/1317	(C–C) υ
18	A′	1260m	–	1404	1259	1280/1228	1247/1253	1307/1287	1238/1287	(O–H) δ
19	A′	1250m	1250m	1399	1254	1214/1203	1275/1239	1295/1271	1226/1261	(O–H) δ
20	A′	1230m	–	1371	1230	1161/1153	1219/1245	1252/1237	1252/1237	(C–O) υ
21	A′	1190vs	–	1325	1188	1101/1087	1211/1174	1192/1187	1192/1187	(C–H) δ
22	A′	1170s	1170m	1303	1168	1094/1068	1149/1153	1168/1156	1168/1156	(C–H) δ
23	A′	1135w	–	1256	1126	1084/1064	1138/1149	1165/1138	1165/1138	(C–H) δ
24	A′	1105vs	1105w	1255	1125	1051/1049	1104/1080	1151/1122	1090/1094	(C–H) δ
25	A′	1090vs	–	1207	1082	1027/1019	1078/1101	1131/1117	1071/1089	(C–H) δ
26	A′	1010m	1010vs	1116	1001	1019/993	1019/1023	1061/1035	1005/1009	(C–H) δ
27	A″	980vw	–	1111	996	984/970	984/970	1042/1026	987/1000	(C–H) γ
28	A″	970w	–	1102	988	893/897	982/969	942/937	970/970	(C–H) γ
29	A″	960w	960w	1075	964	856/859	967/962	929/928	957/960	(C–H) γ
30	A″	890m	–	994	891	831/826	873/892	914/907	866/884	(C–H) γ
31	A″	880vs	–	984	882	827/822	868/888	862/849	888/879	(C–H) γ
32	A″	870vs	870w	960	860	759/766	858/858	836/832	861/861	(C–H) γ
33	A′	840vs	–	918	822	744/742	841/831	816/818	840/847	(CCC) δ
34	A′	830m	–	904	810	736/728	832/815	773/769	812/796	(CCC) δ
35	A′	750vs	750vs	812	735	694/696	729/752	761/749	759/743	(CCC) δ
36	A′	740vs	740vs	798	722	666/677	753/731	704/725	725/750	(CCC) δ
37	A′	710w	–	793	717	648/644	732/696	675/683	695/707	(CCC) δ
38	A″	690vs	–	758	686	612/618	692/630	672/668	692/691	(CCC) δ + (O–H) γ
39	A″	650w	–	709	641	610/616	641/665	662/665	627/648	(CCC) δ + (O–H) γ
40	A″	610s	–	676	612	588/586	617/598	635/638	601/622	(O–H) γ
41	A″	570s	–	629	569	543/548	570/564	573/574	573/574	(O–H) γ
42	A″	550s	–	588	532	502/529	567/545	522/547	522/547	(C–C–C) γ
43	A″	490vs	–	546	494	442/433	499/485	456/459	470/475	(C–C–C) γ
44	A″	470s	–	512	463	406/424	459/475	437/456	450/472	(C–C–C) γ
45	A″	460s	460vs	507	458	395/409	446/458	421/446	434/462	(C–C–C) γ
46	A″	450s	450vs	498	450	374/397	423/445	416/416	428/431	(C–C–C) γ
47	A′	440s	440vs	477	431	311/336	351/376	317/341	396/392	(C–C–C) γ
48	A′	410s	–	452	409	277/303	313/339	304/315	380/362	(C–C–C) γ
49	A″	330w	–	368	333	259/278	293/311	273/288	341/331	(C–O) δ
50	A″	300w	300vw	344	311	243/262	275/293	248/267	310/307	(C–O) δ
51	A″	–	280m	311	241	91/151	103/169	92/151	280/279	(C–O) γ
52	A″	240m	–	298	168	49/107	221/235	55/108	167/200	(C–O) γ
53	A″	150m	–	138	138	−461/−410	138/144	−262/−179	157/170	(C–OH) τ
54	A″	130m	–	137	137	−502/−594	115/119	−358/−436	120/131	(C–OH) τ

vs, very strong; s, strong; m, medium; w, weak; as, asymmetric; s, symmetric; υ, stretching; δ, in plane bending; γ, out plane bending; α, deformation; τ, twisting.

and Raman activities calculated by HF and DFT (B3LYP and LSDA) at 6-31+G(d,p) and 6-311+G(d,p) levels with experimental values exposes the variation of IR intensities and Raman activities. In case of IR intensities, the values of HF are found to be higher than DFT (LSDA and B3LYP) levels whereas in the case of Raman activity the effect is reversed. The same effect was also noticed in the earlier work [27]. The comparative graphs of IR intensities and Raman activities for 5 sets are presented Figs. 4 and 5. In this present work for HF very high intensities are observed particularly at frequencies 3510, 1170, 1135 and 470.

4.4. Computed vibrational frequency analysis

The comparative graph of calculated vibrational frequencies by DFT (LSDA/B3LYP) methods 6-31+G(d,p) basis set for the 2,3-ND are given in Fig. 9. From the figure, it is found that the calculated frequencies by LSDA/B3LYP with 6-31+G(d,p) basis set are closer to the experimental frequencies. This observation is in line with earlier work [28].

The standard deviation (SD) calculation mode between experimental and computed frequencies DFT for 2,3-ND is presented in

Table 4
Comparative values of IR intensity and Raman Activity between HF and DFT (LSDA and B3LYP) methods with 6-31+G(d,p) and 6-311+G(d,p) basis sets of 2,3-naphthalenediol.

S. no.	Observed frequency	Calculated with HF/6-31+G(d,p)		Calculated with HF/6-311+G(d,p)		Calculated with LSDA/6-31+G(d,p)		Calculated with LSDA/6-311+G(d,p)		Calculated with B3LYP/6-31+G(d,p)		Calculated with B3LYP/6-311+G(d,p)	
		IR intensity (Ai)	Raman activity (I)	IR intensity (Ai)	Raman activity (I)	IR intensity (Ai)	Raman activity (I)	IR intensity (Ai)	Raman activity (I)	IR intensity (Ai)	Raman activity (I)	IR intensity (Ai)	Raman activity (I)
1	3510	182.2	120.7	104.3	85	164.3	215.1	104.8	149.5	148.0	83.86	178.6	122.7
2	3500	79.84	55.82	133.6	123.6	68.81	68.19	118.2	182.3	49.38	92.71	60.90	173.1
3	3080	18.40	320.15	14.45	326.06	7.45	343.26	3.52	346.6	17.33	12.57	356.8	364.1
4	3070	12.14	45.63	9.96	46.74	1.06	105.98	0.82	98.27	7.70	6.30	63.50	61.39
5	3060	30.28	62.12	24.65	59.47	13.77	67.15	7.87	59.82	29.73	23.89	67.74	61.57
6	3050	7.11	85.65	3.65	87.21	5.56	76.01	3.13	81.85	9.14	4.73	96.98	98.95
7	3040	1.34	54.22	0.27	38.414	1.25	120.63	0.23	100.7	1.31	0.37	71.80	56.47
8	3030	0.04	28.47	0.68	33.14	0.24	26.93	0.03	33.38	0.08	0.10	27.16	33.51
9	1680	1.84	3.21	5.37	1.13	4.83	26.17	2.89	64.27	3.63	4.54	20.74	5.03
10	1630	1.19	78.19	6.11	142.18	1.60	20.96	12.96	45.43	6.68	8.19	5.94	113.5
11	1610	9.03	3.15	44.39	3.69	6.62	6.76	47.50	4.56	1.95	42.45	35.761	3.06
12	1530	58.40	0.90	25.77	1.81	11.07	54.60	18.14	0.44	42.56	19.90	2.45	0.79
13	1460	19.51	58.86	14.99	11.63	58.54	188.61	2.29	43.56	38.76	19.23	283.9	4.46
14	1450	38.28	34.60	6.38	1.95	17.64	10.26	41.22	107.1	0.53	4.43	5.00	5.91
15	1390	6.02	255.5	83.86	104.95	0.70	1.87	9.08	10.62	54.09	16.32	1.78	179.1
16	1365	27.40	8.40	11.05	149.74	68.32	20.73	2.55	0.42	0.26	19.23	13.75	0.96
17	1330	54.47	7.88	31.92	17.12	3.11	0.94	11.37	0.77	6.49	1.72	1.04	0.91
18	1260	55.58	0.75	16.26	0.97	102.38	3.72	91.1	3.26	63.00	0.17	0.95	0.65
19	1250	57.14	1.63	85.95	3.31	3.25	0.24	6.33	0.49	10.46	64.84	0.23	1.60
20	1230	59.74	5.89	32.74	3.03	73.57	1.13	14.20	0.25	89.95	21.06	2.11	0.19
21	1190	0.01	5.29	18.22	7.16	6.17	1.11	24.06	11.29	16.41	46.58	1.18	16.33
22	1170	114.0	4.09	131.2	4.67	11.86	6.97	0.07	2.86	0.56	10.32	2.71	4.68
23	1135	187.4	5.10	128.6	16.2	0.49	2.40	12.50	10.79	5.87	8.78	6.13	2.79
24	1105	24.83	8.31	30.3	8.9	24.94	9.07	23.15	4.59	37.32	221.1	6.33	15.78
25	1090	16.47	1.46	47.7	3.9146	197.5	11.59	265.2	21.10	264.7	87.70	9.44	10.25
26	1010	0.32	22.40	1.46	38.67	11.75	25.04	17.68	37.34	5.45	3.67	25.75	35.77
27	980	48.89	1.46	0.002	1.25	124.3	0.28	78.40	3.82	75.13	67.22	0.59	0.30
28	970	0.01	0.96	6.04	1.79	3.67	0.03	7.70	0.72	0.02	0.00	0.16	0.18
29	960	5.18	2.14	1.25	2.57	0.03	0.07	0.00	0.09	4.60	7.33	0.02	0.12
30	890	9.19	0.10	12.06	0.06	27.91	15.55	6.95	0.91	5.10	5.57	1.13	0.86
31	880	58.34	2.73	41.45	3.15	8.16	2.37	18.83	24.96	36.99	24.98	18.31	27.30
32	870	18.01	1.45	19.28	2.73	8.10	1.16	0.82	1.11	31.10	25.30	1.83	2.31
33	840	5.48	0.36	10.51	0.83	54.76	12.72	47.18	3.26	21.33	25.31	1.25	1.28
34	830	36.20	17.96	24.21	25.57	58.85	6.74	47.64	17.79	6.74	7.75	0.24	0.30
35	750	56.44	0.62	20.87	0.96	9.36	0.43	30.28	2.36	63.23	45.70	20.00	21.98
36	740	59.69	21.74	30.84	0.82	0.44	0.04	0.19	0.02	0.65	0.73	0.16	0.07
37	710	2.58	0.90	45.82	26.64	15.69	0.39	17.91	0.99	34.15	33.32	0.54	0.78
38	690	5.84	0.36	15.63	0.73	4.17	0.65	17.67	0.76	9.19	21.90	0.30	1.73
39	650	15.38	0.19	10.93	0.30	12.21	0.18	9.22	0.29	11.91	18.11	0.77	0.71
40	610	9.59	0.44	10.13	0.60	20.88	0.26	26.51	1.65	8.51	8.22	0.30	0.37
41	570	17.59	5.05	9.13	5.41	32.48	4.72	13.70	2.92	23.93	12.37	4.64	3.63
42	550	1.81	0.02	1.45	0.10	2.96	0.27	4.49	0.31	1.46	2.39	0.09	0.10
43	490	64.55	1.95	136.20	1.01	4.85	22.30	4.69	26.31	4.96	15.72	21.12	2.40
44	470	111.7	2.80	4.82	4.47	9.05	2.12	7.44	2.41	16.22	18.90	1.65	1.44
45	460	44.41	1.99	15.05	0.83	7.31	3.33	44.96	0.51	12.39	5.85	1.37	25.25
46	450	52.03	0.89	77.80	7.43	39.84	0.16	5.00	4.30	4.07	1.34	3.94	5.38
47	440	9.44	18.49	33.74	19.43	0.23	0.14	5.76	0.49	0.83	3.81	0.13	0.29
48	410	3.28	5.21	4.27	7.16	5.01	0.39	5.01	0.72	2.03	3.84	0.27	0.68
49	330	0.41	0.32	2.31	0.15	2.96	0.18	0.95	0.56	2.96	0.69	0.24	0.56
50	300	8.20	0.25	5.65	0.74	2.44	0.39	8.03	0.74	0.95	4.47	0.42	0.67
51	280	1.91	0.29	1.94	0.64	0.12	0.80	3.78	0.82	0.10	2.09	0.85	0.93
52	240	0.41	0.52	1.26	0.73	2.16	0.64	0.80	0.92	0.96	0.52	0.82	0.95
53	150	0.30	0.76	1.10	0.87	65.35	3.60	116.0	3.99	73.30	111.9	2.65	3.09
54	130	0.52	0.82	0.21	0.80	184.5	2.80	108.0		171.5	105.0	2.19	2.39

Table 5
Standard deviation of frequencies computed by HF and DFT (LSDA/B3LYP) at 6-31+G(d,p) and 6-311+G(d,p) basis sets.

S. no.	Basic set levels	Total values	Average	Standard deviation average	Deviation ratio
	Experimental	65,865	1219.72		
1	HF/6-31+G(d,p)	72,872	1428.86	104.36	
2	LSDA/6-31+G(d,p)	66,456	1303.05	78.37	1.331
3	B3LYP/6-31+G(d p)	68,182	1336.90	66.42	1.179
4	LSDA/6-311+G(d,p)	64,614	1281.19	68.27	0.972
5	B3LYP/6-311+G(d,p)	67,067	1315.03	48.36	1.411

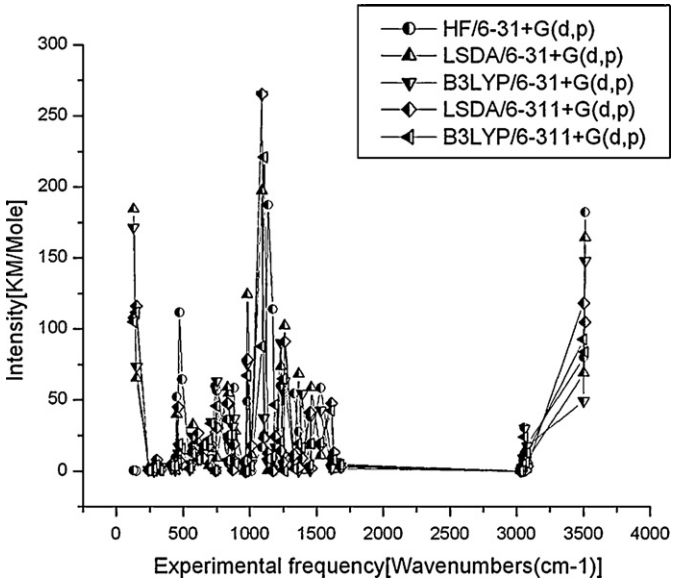

Fig. 4. Comparative graph of IR intensities by HF and DFT[LSDA/B3LYP].

Table 5. According to the standard deviation the computed frequency deviation increase in going from B3LYP/6-31+G(d,p) to B3LYP/6-311+G(d,p) to LSDA/6-311+G(d,p) to LSDA/6-31+G(d,p) to HF/6-31+G(d,p). The deviation ratio between HF/6-31+G(d,p) and LSDA/6-31+G(d,p) is 1.331, B3LYP/6-31+G(d,p) is 1.179, and LSDA/6-311+G(d,p) is 0.972 and B3LYP/6-311+G(d,p) is 1.411. It is also observed that the calculated frequencies by B3LYP/6-311+G(d,p) basis set are close to the experimental frequencies than other basis set in DFT method.

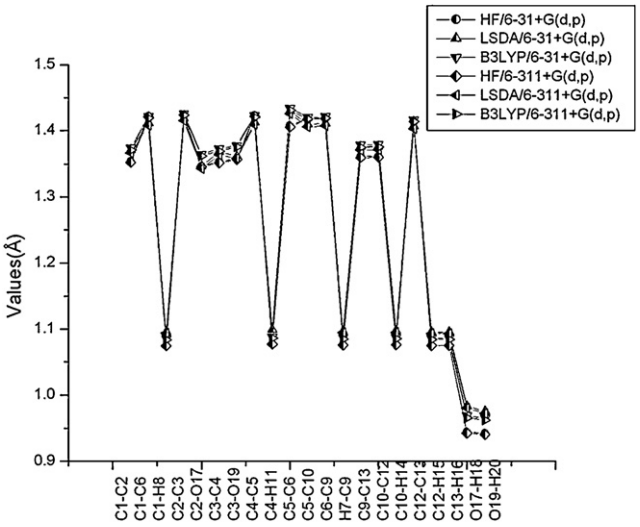

Fig. 6. Bond length differences between theoretical [HF/DFT] approaches.

4.5. Ideal frequency estimation analysis

For 2,3-ND group the vibrational modes are C–H stretch, C=C stretch, O–H stretch and C–O stretch. The ideal estimation of frequencies by DFT (LSDA/B3LYP) methods are presented in Table 6. The frequencies calculated by various basis sets exactly coincide with experimentally observed values of FT-IR and FT-Raman without scaling while comparing the estimation of frequencies by various sets of the DFT method, the B3LYP/6-311+G(d,p) basis sets estimate accurately more number of frequencies than other

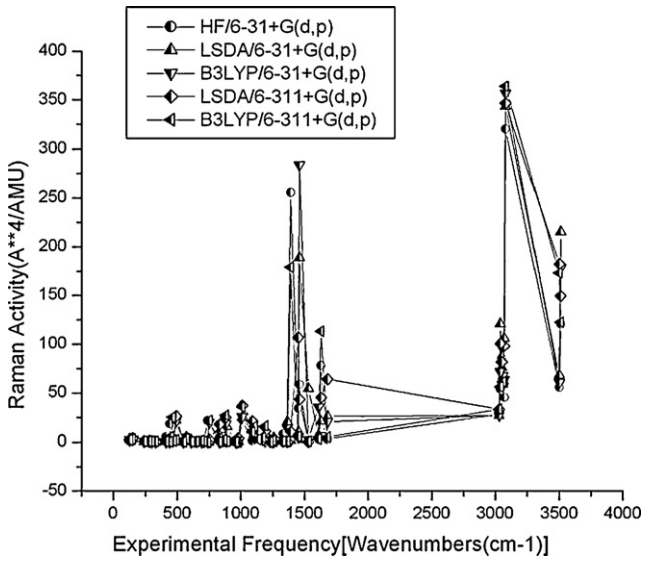

Fig. 5. Comparative graph of Raman activities by HF and DFT (LSDA/B3LYP).

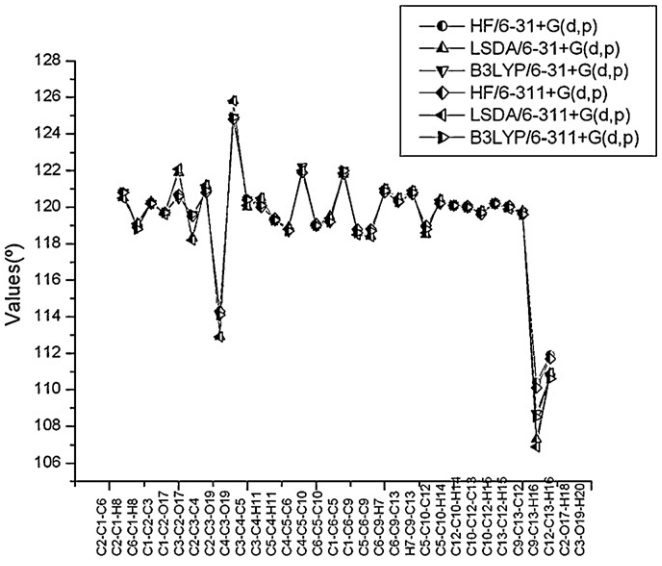

Fig. 7. Bond angle differences between theoretical [HF/DFT] approaches.

Table 6
Ideal estimation of calculated frequencies by DFT (LSDA/6-311+G(d,p), B3LYP/6-31+G(d,p) and B3LYP/6-311+G(d,p)) basis sets.

S. No.	Basis sets					
	LSDA 6-311+G(d,p)	Assigned frequencies	B3LYP 6-31+G(d,p)	Assigned frequencies	B3LYP 6-311+G(d,p)	Assigned frequencies
1	1610	(C=C) υ	1252	(C–O) υ	1317	(C–C) υ
2	1519	(C=C) υ	1192	(C–H) δ	1287	(O–H) υ
3	1449	(C–C) υ	1168	(C–H) δ	1237	(C–O) υ
4	1383	(C–C) υ	1165	(C–H) δ	1187	(C–H) δ
5	1317	(C–C) υ	573	(O–H) υ	1156	(C–H) δ
6	970	(C–C) υ	522	(C–C–C) υ	1138	(C–H) δ
7					574	(O–H) υ
8					547	(C–C–C–) υ

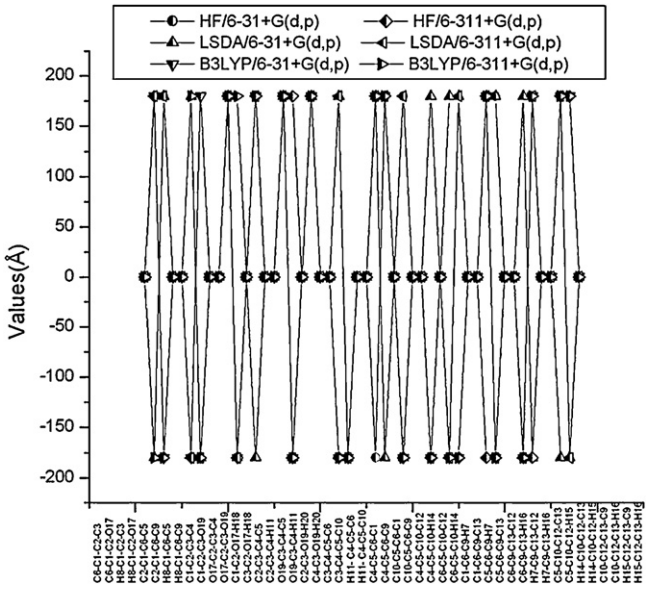

Fig. 8. Dihedral angle difference between theoretical [HF and DFT] approaches.

sets. The estimated frequencies belong to both finger print and functional group region. The B3LYP/6-311+G(d,p) set gives the frequencies accurately for C–C, O–H, C–O stretching, C–H in-plane bending, O–H, CCC out of plane bending vibrations where as the LSDA/6-311+G(d,p) set yields the frequencies accurately for C–C stretching and C–H out of plane bending. The B3LYP/6-31+G(d,p) set gives the frequencies accurately for C–O stretching, C–H in-plane bending and O–H, C–C–C out of plane bending vibration.

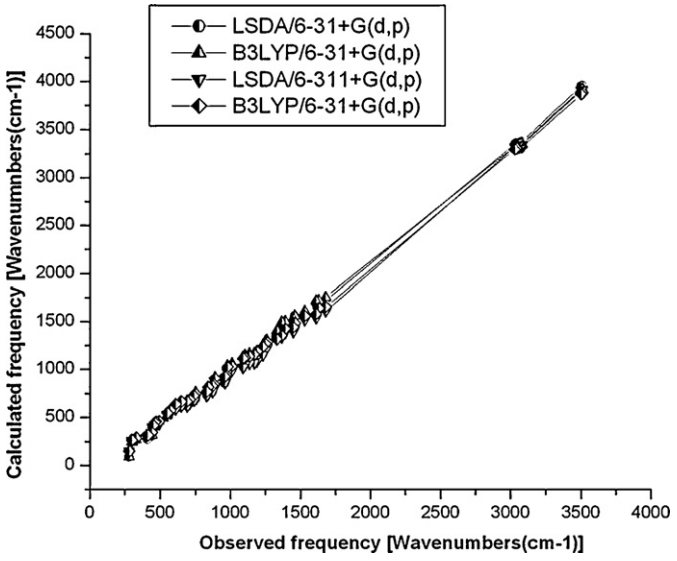

Fig. 9. Comparative graph of experimental and computed frequencies by DFT.

4.5.1. C–H vibrations

The hetero aromatic organic compounds commonly exhibit multiple weak bands in the region 3200–3000 cm^{-1} due to C–H stretching vibrations [29–31]. In pure naphthalene the same has occurred in the region 3080–3000 cm^{-1} [10]. The frequency of 2-napthalenol has appeared in the region 3085–3040 cm^{-1} [32,33]. In the present compound, the scaled vibrations, mode nos.: 3–8, correspond to the stretching mode of C1–H8, C4–H11, C9–H7, C10–H14, C13–H16 and C12–H15 units. In the title molecule, the bands have been observed at 3080w, 3060w, 3050w and 3040w cm^{-1} (FT-IR) and 3070vs, 3060vs, 3040vs, 3030w cm^{-1} (FT-Raman) to C–H ring stretching vibrations. The scaled values computed by B3LYP/6-31+G(d,p) and HF/6-311+G(d,p) levels coincides well with the experimental observation. The C–H in-plane ring bending vibrations normally occurred as a number of strong to weak intensity sharp bands in the region 1300–1000 cm^{-1} [34,35]. The bands for C–H in-plane bending vibrations of the title compound identified at 1190vs, 1170s, 1135w, 1105vs, 1090vs, 1010m cm^{-1} (FT-IR) and 1170m, 1105w, 1010vs cm^{-1} (FT-Raman). The theoretically compound frequencies for C–H in-plane bending vibrations by B3LYP 6-31+G(d,p)/6-311+G(d,p) methods shows excellent agreement with recorded spectrum as well as literature data.

The C–H out-of-plane bending vibrations are strong coupled vibrations and normally observed in the region 960–810 cm^{-1} [36–40]. Most of the vibrations are observed in the Raman spectrum except two. In the present case, the bands are identified at 980vw, 970w, 960w, 890m, 880vs, 870vs cm^{-1} (FT-IR) and 960w, 870w cm^{-1} (FT-Raman) for C–H out-of-plane bending. Except first two bands the assigned frequencies are found to be well within their characteristic regions. The change in the frequencies of these deformations from the values in naphthalene is almost determined exclusively by the relative position of the substituents and is almost independent of their nature.

4.5.2. C=C vibrations

Generally the C=C stretching vibrations in aromatic compounds are seen in the region of 1430–1650 cm^{-1} [41]. Naphthalene ring stretching vibrations are expected in the region 1620–1390 cm^{-1} [42]. According to Socrates [34], the presence of conjugate substituent such as C=C causes a heavy doublet formation around the region 1625–1575 cm^{-1}. The six ring carbon atoms undergo coupled vibrations, called skeletal vibrations and give a maximum of four bands in the region 1660–1420 cm^{-1} [43]. As predicted in the earlier references, the prominent peaks at 1680vw, 1630s, 1610s, 1530vs cm^{-1} (FT-IR) and 1630w, 1610w cm^{-1} (FT-Raman) are due to strong C=C stretching. Ring C–C stretching vibrations normally occur in the region 1590–1430 cm^{-1} [44]. The present case, the C–C stretching vibrations have been observed at 1460vs, 1450vs,

Table 7
Theoretical electronic absorption spectra of 2,3-naphthalenediol (absorption wavelength λ (nm), excitation energies *E* (eV) and oscillator strengths (*f*)) using TD-DFT/B3LYP/6-311G(d,p) method in gas and solvent (DMSO and chloroform) phase.

DMSO			Chloroform			Gas			Gas	
λ (nm)	*E* (eV)	(*f*)	λ (nm)	*E* (eV)	(*f*)	λ (nm)	*E* (eV)	(*f*)	Major contribution[a]	Assignment
291.59	4.2519	0.0656	292.23	4.2427	0.0707	292.14	4.2440	0.0482	H → L (50%), H−1 → L (26%)	π–π*
285.71	4.3395	0.0498	285.33	4.3453	0.0489	282.65	4.3864	0.0297	H → L (42%), H−1 → L (41%)	π–π*
223.59	5.5452	1.2602	223.94	5.5365	1.2761	229.08	5.4123	0.0004	H → L+2 (96%)	π–π*

[a] H: HOMO; L: LUMO.

1390vs, 1365vs, 1330m cm^{-1} (FT-IR) and 1460w, 1365vs cm^{-1} (FT-Raman). When compared to the literature range cited, above, there is a considerable decrease in frequencies which is also worsening with the increase of mass of substitutions. The peaks are observed at 840, 830, 750, 740, 710, 690 and 650 cm^{-1} due to C–C–C in-plane bending vibrations and the peaks at 550, 490, 470, 460, 450, 440 and 410 cm^{-1} are due to C–C–C out-of-plane bending vibrations these assignments are in line with the assignments proposed by the literature [45–47].

4.5.3. O–H vibration

The OH group gives rise to three vibrations-stretching, out-of-plane bending and in-plane deformations. The relative intensity of the band due to the hydroxyl stretching vibration decreases with increase in concentration, with additional broader bands appearing at lower frequencies 3580–3200 cm^{-1}. These bands are the result of the presence of intermolecular bonding, the amount of which increases with concentration [34]. In this present work the O–H stretching vibration observed at 3510vs, 3500vs cm^{-1} (FT-IR) and 3510, 3500 cm^{-1} (FT-Raman).

The in-plane OH deformation vibration gives rise to a strong band in the region 1440–1260 cm^{-1}. In concentrated solutions, this band is very broad, extending over approximately 1500–1300 cm^{-1}. In this present work the O–H in-plane bending vibration assigned at 1390, 1260 and 1250 cm^{-1}. The OH out-of-plane vibration gives a broad band in the region 700–600 cm^{-1}. The position of this band is dependent on the strength of the hydrogen bond. In this present work the OH out-of-plane bending vibration occurs at 690vs, 650w, 610s and 570s cm^{-1}.

4.5.4. C–O vibration

In phenol, the C–O stretching vibration occurs at 1270 cm^{-1} in gas phase and 1268 cm^{-1} in solid phase [48]. Buyukmurat and Akyuz [49] have assigned the strong absorption band in the Raman spectrum at 1314 cm^{-1} corresponds to C–O stretching vibration. In accordance with the above observations the C–O stretching vibration in 2,3-ND has been identified at 1230 cm^{-1}. The CO stretching vibration in the mode (no. 20), with HF/6-31+G(d,p) and B3LYP/6-311+G(d,p) predicated frequency of 1230 and 1237 cm^{-1} (Table 3). This is in excellent agreement with experimental frequency. The C–O in-plane bending observed at 330 and 300 cm^{-1} and the out-of-plane bending assigned at 280 and 240 cm^{-1}.

4.6. UV–vis spectra analysis

In the UV–vis region with high extinction coefficients, all molecules allow strong π–π* and σ–σ* transition [50]. Ultraviolet spectra analyses of 2,3-ND have been investigated by theoretical calculation. In order to understand electronic transitions of compound, TD-DFT calculations on electronic absorption spectra in gas phase and solvent (DMSO and Chloroform) are performed. The calculated Frontier orbital energies, absorption wavelengths (λ), oscillator strengths (*f*) and excitation energies (*E*) for gas phase and solvent (DMSO and chloroform) are illustrated in Table 7. The major contributions of the transitions were designated with the aid of SWizard program [51]. Calculations of the molecular orbital geometry show that the visible absorption maxima of this molecule correspond to the electron transition between Frontier orbitals such as translation from HOMO to LUMO. As can be seen from the Table 7, the calculated absorption maxima values have been found to be 292.14, 282.65, 229.08 nm for gas phase, 291.59, 285.71, 223.59 nm for DMSO solution and 292.23, 285.33, 223.94 nm for chloroform solution at DFT/B3LYP/6-311G(d,p) method. As can be seen, all calculations performed are very close. In view of calculated absorption spectra, the maximum absorption wavelength corresponds to the electronic transition from HOMO to LUMO with 50% and from HOMO−1 to LUMO with 26% contribution. This transition is predicted as π–π* transition. The other wavelength, excitation energies, oscillator strength, calculated counterparts with major contributions and assignments can be seen in Table 7.

4.7. HOMO–LUMO analysis

The total energy, energy gap and dipole moment have influence on the stability of a molecule. We have performed optimization in order to investigate the energetic behavior and dipole moment of title compound in solvent and gas phase. The total energy, dipole moment and Frontier molecular orbital energies have been calculated with B3LYP/6-311G(d,p) level. Results obtained in solvent and gas phase are listed in Table 8.

HOMO and LUMO are very important parameters for chemical reaction. We can determine the way the molecule interacts with other species; hence, they are called the Frontier orbitals. The HOMO is the orbital that primarily acts as an electron donor and the LUMO is the orbital that largely acts as the electron acceptor, and the gap between HOMO and LUMO characterizes

Table 8
Calculated energies values of 2,3-naphthalenediol in gas and solvent (DMSO and chloroform) phase.

TD-DFT/B3LYP/6-311G(d,p)	DMSO	Chloroform	Gas
E_{total} (hartree)	−536.32656686	−536.32406656	−536.31740882
E_{HOMO} (eV)	−5.94492	−5.88750	−5.77729
E_{LUMO} (eV)	−1.18343	−1.13391	−1.04601
$\Delta E_{HOMO-LUMO\ gap}$ (eV)	4.76149	4.75359	4.73128
E_{HOMO-1} (eV)	−6.18737	−6.14438	−6.07417
E_{LUMO+1} (eV)	−0.30096	−0.24409	−0.13932
$\Delta E_{HOMO-1-LUMO+1\ gap}$ (eV)	5.88641	5.90029	5.93485
Dipole moment	3.4101	3.1574	2.6011

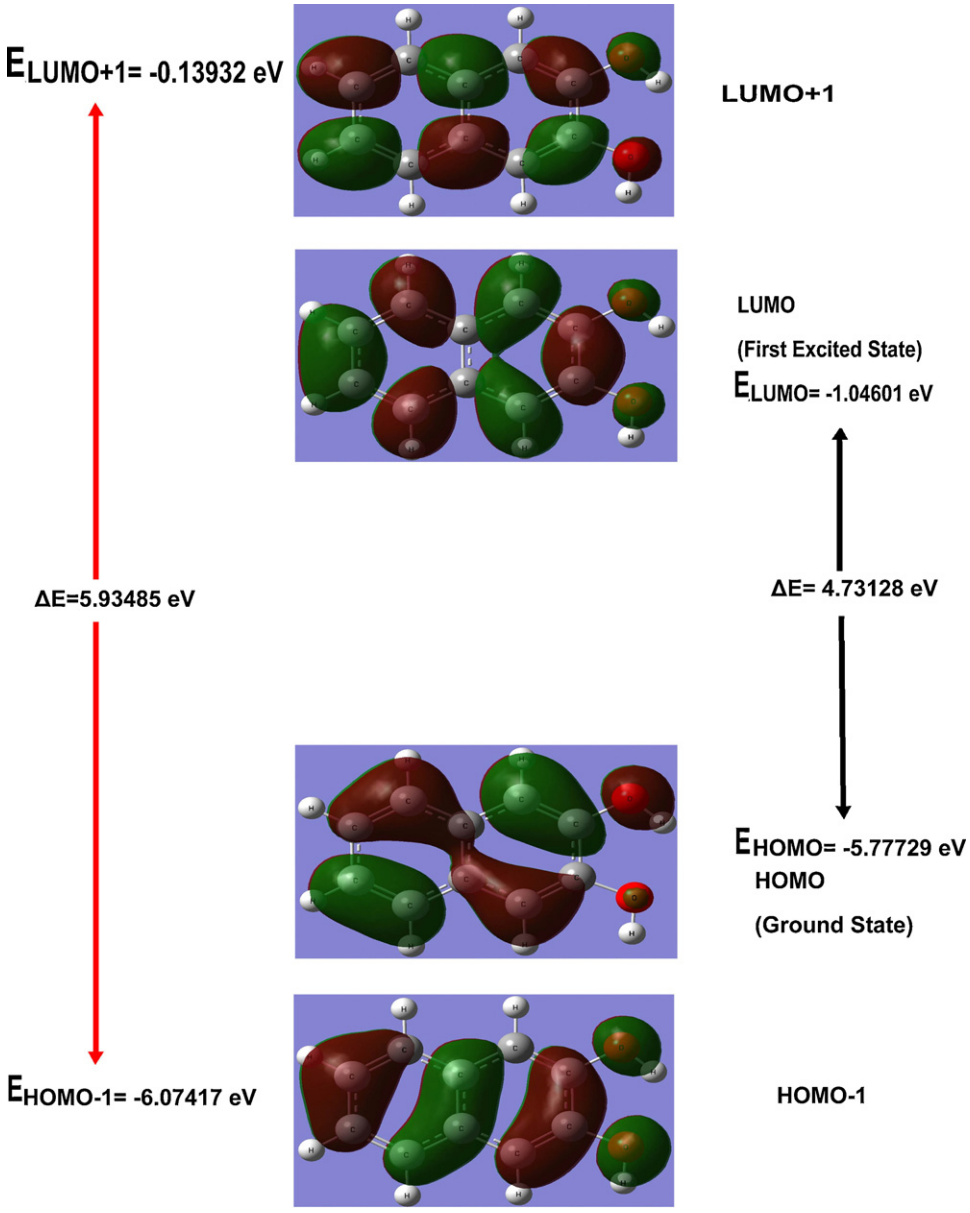

Fig. 10. The atomic orbital compositions of the Frontier molecular orbital for 2,3-naphthalenediol molecule.

the molecular chemical stability [52]. The energy gap between the highest occupied and the lowest unoccupied molecular orbitals, is a critical parameter in determining molecular electrical transport properties because it is a measure of electron conductivity. The energy values of HOMO are computed −5.94492, −5.88750 and −5.77729 eV and LUMO are −1.18343, −1.13391 and −1.04601 eV, and the energy gap values are 4.76149, 4.75359 and 4.73128 eV in DMSO, chloroform and gas phase for 2,3-ND molecule, respectively. Surfaces for the Frontier orbitals were drawn to understand the bonding scheme of present compound. We examine the four important molecular orbitals (MO) for title molecule: the second highest and highest occupied MOs and the lowest and the second lowest unoccupied MOs which we denote HOMO−1, HOMO, LUMO and LUMO+1, respectively. These MOs for gas phase are outlined in Fig. 10. The positive phase is red and the negative one is green. According to Fig. 10, the HOMO of 2,3-ND presents a charge density localized on the ring and expect of OH group, but LUMO is characterized by a charge distribution on all molecule expect of hydrogen atoms in OH group. Moreover lower in the HOMO and LUMO energy gap explains the eventual charge transfer interactions taking place within the molecule.

Dipole moment reflects the molecular charge distribution and is given as a vector in three dimensions. Therefore, it can be used as descriptor to depict the charge movement across the molecule. Direction of the dipole moment vector in a molecule depends on the centres of positive and negative charges. Dipole moments are strictly determined for neutral molecules. We can say that in going from the gas phase to the solvent phase, the dipole moment value increases (Table 8).

4.8. Thermodynamic properties

On the basis of vibrational analysis at B3LYP/6-311G (d,p) level, the standard statistical thermodynamic functions: standard heat capacities ($C^0_{p,m}$) standard entropies (S^0_m), and standard enthalpy changes (ΔH°_m) for the title compounds were obtained from the theoretical harmonic frequencies and listed in Table 9.

Table 9
Thermodynamic properties at different temperatures at the B3LYP/6-311+G(d,p) level for 2,3-naphthalenediol molecule.

T (K)	$C^0_{p,m}$ (cal mol^{-1} K^{-1})	S^0_m (cal mol^{-1} K^{-1})	ΔH°_m(kcal/mol)
100	12.506	65.865	1.011
150	18.755	72.900	1.890
200	25.377	79.770	3.091
250	32.054	86.595	4.627
298.15	38.340	93.132	6.418
300	38.576	93.382	6.493
350	44.755	100.104	8.677
400	50.461	106.724	11.159
450	55.632	113.205	13.913
500	60.265	119.520	16.912
550	64.393	125.651	20.130
600	68.068	131.587	23.542
650	71.347	137.327	27.129
700	74.284	142.871	30.871

From Table 9, it can be observed that these thermodynamic functions are increasing with temperature ranging from 100 to 700 K due to the fact that the molecular vibrational intensities increase with temperature [53]. The correlation equations between heat capacities, entropies, enthalpy changes and temperatures were fitted by quadratic formulas and the corresponding fitting factors (R^2) for these thermodynamic properties are 0.9995, 1.0000 and 0.9998, respectively. The corresponding fitting equations are as follows and the correlation graphics of those shows in Figs. 11–13.

$$C^0_{p,m} = -4.4221 + 0.1677T - 7.8308 \times 10^{-5}T^2 \quad (R^2 = 0.9995)$$

$$S^0_m = 50.9695 + 0.1496T - 2.5673 \times 10^{-5}T^2 \quad (R^2 = 1.0000)$$

$$\Delta H^\circ_m = -0.5160 + 0.0078T + 5.3453 \times 10^{-5}T^2 \quad (R^2 = 0.9998)$$

All the thermodynamic data supply helpful information for the further study on the 2,3-ND. They can be used to compute the other thermodynamic energies according to relationships of thermodynamic functions and estimate directions of chemical reactions according to the second law of thermodynamics in thermochemical field [54]. Notice: all thermodynamic calculations were done in gas phase and they could not be used in solution.

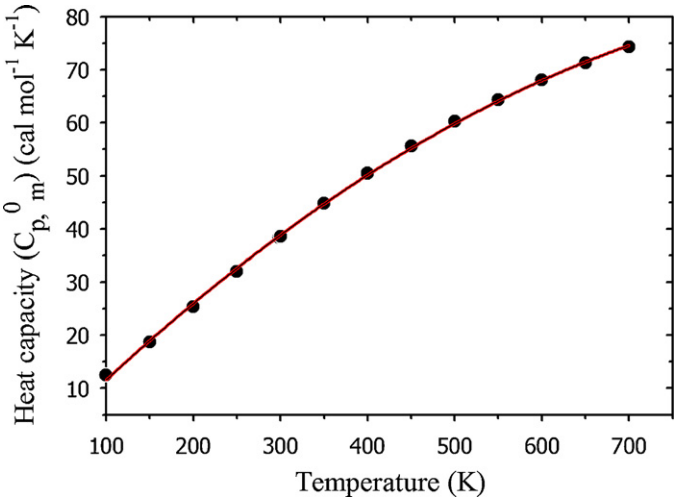

Fig. 11. Correlation graphic of heat capacity and temperature for 2,3-naphthalenediol molecule.

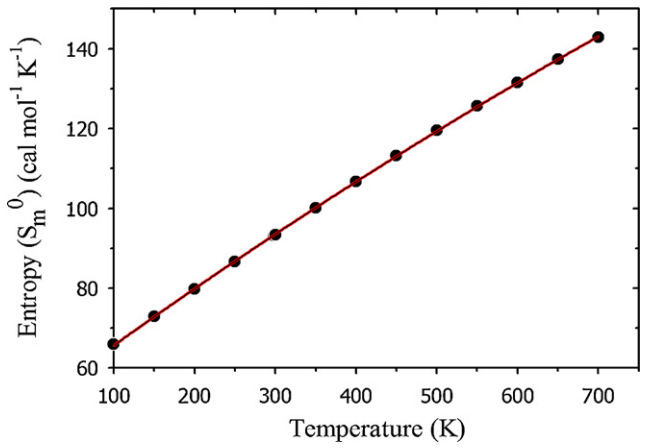

Fig. 12. Correlation graphic of entropy and temperature for 2,3-naphthalenediol molecule.

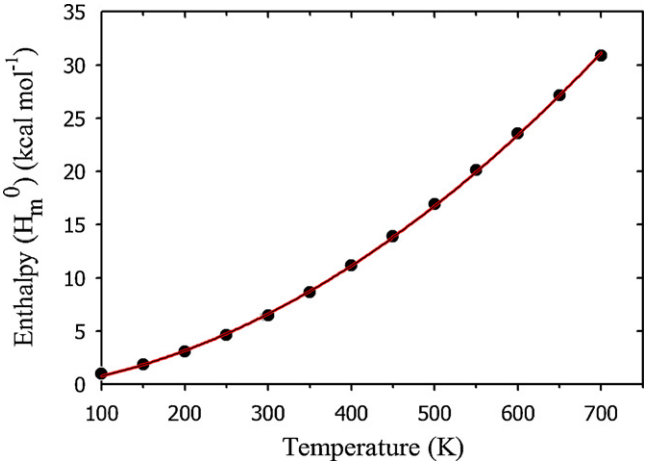

Fig. 13. Correlation graphic of enthalpy and temperature for 2,3-naphthalenediol molecule.

5. Conclusion

Attempts have been made in the present work for the molecular parameters and frequency assignments for the compound 2,3-naphthalenediol from the FT-IR and FT-Raman spectra. Vibrational frequencies, infrared intensities and Raman activities are calculated and analyzed by HF and DFT(LSDA/B3LYP) levels of theory utilizing 6-31+G(d,p) and 6-311+G(d,p) basis sets. Based on calculated energy differences, the C1 conformer is found to be most the stable conformer and C3 conformer is predicted the unstable conformer. The difference between the observed and scaled wave number values of most of fundamental is very small. Comparison between the calculated and experimental structural parameters indicated that B3LYP results are in good agreement with experimental values. On the basis of agreement between the calculated and observed results, assignments of fundamental vibrational modes of 2,3-ND are examined. Therefore, the assignments made at higher level of theory with basis set with only reasonable deviations from the experimental values seem to be correct. The optimized geometry parameters calculated at B3LYP/6-31+G(d,p)/6-311+G(d,p) are slightly larger than those calculated at HF/6-31+G(d,p)/6-311+G(d,p) level and the HF calculated values coincides well compared with the experimental data. The lowering of the HOMO–LUMO energy gap value has substantial influence on the intramolecular charge transfer and bioactivity of the molecule. The correlations between the statistical

thermodynamics and temperature are also obtained. It is seen that the heat capacities, entropies and enthalpies increase with the increasing temperature owing to the intensities of the molecular vibrations increase with increasing temperature.

References

[1] R.G. Parr, W. Yang, Density Functional Theory of Atoms and Molecules, Oxford, New York, 1989.
[2] E.B. Wilson Jr., J.C. Decius, P.C. Cross, Molecular Vibrations, McGra-Hill, New York, 1955.
[3] R.O. Jones, O. Gunnarson, Rev. Mol. Phys. 61 (1989) 689.
[4] P. Pulay, G. Fogarasi, X. Zhou, P.W. Taylor, Vib. Spectrosc. 1 (1990) 159.
[5] Z. Zhengyu, F. Aiping, D.U. Dongmeim, Int. J. Quant. Chem. 78 (2000) 247.
[6] http://www.wikypedia.com.
[7] A. Srivastava, V.B. Singh, Ind. J. Pure Appl. Phys. 45 (2007) 714–720.
[8] J. Xavier, V. Balachandran, M. Arivazhagan, G. Ilango, Ind. J. Pure Appl. Phys. 48 (2010) 245–250.
[9] P.B. Nagabalasubramanian, S. Periandy, Spectrochim. Acta A 77 (2010) 1099.
[10] M. Govindarajan, K. Ganasan, S. Periandy, M. Karabacak, Spectrochim. Acta A: Mol. Biomol., Spect. 79 (2011) 646–653.
[11] G. Fogarasi, P. Pulay, J.R. During (Eds.), Vibrational Spectra and Structure, vol. 14, Elesevier, Amsterdam, 1985.
[12] A.D. Becke, Phys. Rev. A 38 (1988) 3098.
[13] C. Lee, W. Yang, R.G. Parr, Phys. Rev. B 37 (1988) 785.
[14] A.D. Becke, J. Chem. Phys. 98 (1993) 5648.
[15] Z. Zhengyu, D. Dongmei, J. Mol. Struct. (Theochem.) 505 (2000) 247–249.
[16] Y. Carissan, W. Klopper, J. Mol. Struct. (Theochem.) 940 (2010) 115–118.
[17] M.H. JamroAz, J.C. Dobrowolski, J. Mol. Struct. 565–566 (2001) 475–480.
[18] T. Clar, J. Chadrasekhar, G.W. Spitznagel, P.V.R. Schleyer, J. Comput. Chem. (1983) 294.
[19] M.J. Frisch, J.A. Pople, J.S. Binkley, J. Chem. Phys. 80 (1984) 3265.
[20] M. Karabacak, D. Karagoz, M. Kurt, Spectrochim. Acta A 72 (2009) 1076.
[21] M.J. Frisch, A.B. Nielsen, A.J. Holder, Gauss View Users Manual, Guassian Inc., Pittsburgh, PA, 2004.
[22] Gaussian 09 Program, Guassian Inc., Wallingford, CT, 2009.
[23] F. Pauzat, D. Talbi, M.D. Miller, J. Phys. Chem. 96 (1992) 7882.
[24] S. Kashino, M. Tomita, M. Haisa, Acta Crystallogr. C 44 (1988) 730.
[25] J.V. Prasad, S.B. Rai, S.N. Thakur, Chem. Phys. Lett. 164 (1989) 629.
[26] M.K. Ahmed, B.R. Henry, J. Phys. Chem. (1737) 1986.
[27] S. Ramalingam, S. Periandy, M. Govindarajan, S. Mohan, Spectrochim. Acta A 75 (2010) 1308–1314.
[28] S. Ramalingam, S. Periandy, B. Narayanan, S. Mohan, Spectrochim. Acta A 76 (2010) 84–92.
[29] V. Krishnakumar, V. Balachandran, T. Chithambarathann, Spectrochim. Acta A 62 (2005) 918–925.
[30] W.O. George, P.S. Mcintyre, Infrared Spectroscopy, John Wiley & Sons, London, 1987.
[31] J. Coates, R.A. Meyers, Interpretation of Infrared Spectra: A Practical Approach, John Wiley and Sons Ltd., Chichester, 2000.
[32] M.H. Jamroz, J.C. Dobrowolski, R. Brzozowski, J. Mol. Struct. 787 (2006) 172.
[33] V. Chis, M. Oltean, A. Pirnau, V. Miclaus, S. Filip, J. Optoelectron. Adv. Mater. 8 (3) (2006) 1143.
[34] G. Socrates, Infrared and Raman Characteristics Group Frequencies, 3rd ed., Wiley, New York, 2001.
[35] N. Sundaraganesan, H. Saleem, S. Mohan, M. Ramalingam, V. Sethuraman, Spectrochim. Acta A 62 (2005) 740–751.
[36] V.K. Kumar, N. Prabavathi, Spectrochim. Acta A 71 (2008) 449–457.
[37] A. Altun, K. Golcuk, M. Kumru, J. Mol. Struct. (Theochem.) 637 (2003) 155.
[38] S.J. Singh, S.M. Pandey, Ind. J. Pure Appl. Phys. 12 (1974) 300–304.
[39] Y. Sun, Q. Hao, Z. Yu, W. Jiang, L. Lu, X. Wang, Spectrochim. Acta A 73 (2009) 892–901.
[40] N. Sundaraganesan, B.D. Joshua, T. Rajakumar, Ind. J. Pure Appl. Phys. 47 (2009) 248–258.
[41] V. Krishnakumar, N. Surumbarkuzhali, S. Muthunatesan, Spectrochim. Acta A 71 (2009) 1810–1813.
[42] S. Chandra, H. Saleem, N. Sundaraganesan, S. Sebastian, Spectrochim. Acta A 74 (2009) 704–713.
[43] V.R. Dani, Organic Spectroscopy, Tata-MacGraw Hill Publishing Company, New Delhi, 1995.
[44] S. Periandy, S. Mohan, Proc. Natl. Acad. Sci. Ind. 68A (III) (1998).
[45] A. Hussein, K. Howard, J. Mol. Struct. (GB) 42 (1977) 37.
[46] M. Karabacak, D. Karagöz, M. Kurt, J. Mol. Struct. 892 (2008) 25.
[47] M. Karabacak, M. Kurt, A. Atac, J. Phys. Org. Chem. 22 (2009) 321.
[48] A.J. Abkowicz-Bienko, Z. Latajka, D.C. Bienko, D. Michalska, Chem. Phys. 250 (1999) 123.
[49] Y. Buyukmurat, S. Akyuz, J. Mol. Struct. 744 (2005) 921.
[50] A. Coruh, F. Yilmaz, B. Sengez, M. Kurt, M. Cinar, M. Karabacak, Struct. Chem. 22 (2011) 45–56.
[51] S.I. Gorelsky, SWizard Program Revision 4.5, University of Ottawa, Ottawa Canada, 2010, http://www.sg.chem.net/.
[52] K. Fukui, Science 218 (1982) 747.
[53] J. Bevan Ott, J. Boerio-Goates, Calculations from Statistical Thermodynamics, Academic Press, 2000.
[54] R. Zhang, B. Dub, G. Sun, Y. Sun, Spectrochim. Acta A 75 (2010) 1115–1124.